JACS
JOURNAL OF THE AMERICAN CHEMICAL SOCIETY

Subscriber access provided by ISTANBUL TEKNIK UNIV

Article

Water Activity Regulates the Q_A^- to Q_B Electron Transfer in Photosynthetic Reaction Centers from *Rhodobacter sphaeroides*

Gerardo Palazzo, Francesco Francia, Antonia Mallardi,
Mauro Giustini, Francesco Lopez, and Giovanni Venturoli

J. Am. Chem. Soc., **2008**, 130 (29), 9353-9363 • DOI: 10.1021/ja801963a • Publication Date (Web): 25 June 2008

Downloaded from http://pubs.acs.org on February 8, 2009

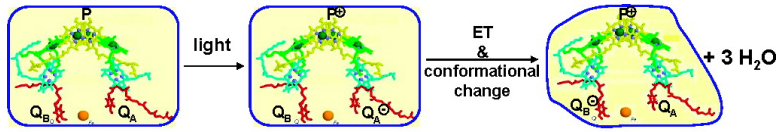

More About This Article

Additional resources and features associated with this article are available within the HTML version:

- Supporting Information
- Access to high resolution figures
- Links to articles and content related to this article
- Copyright permission to reproduce figures and/or text from this article

View the Full Text HTML

ACS Publications
High quality. High impact.

Journal of the American Chemical Society is published by the American Chemical Society. 1155 Sixteenth Street N.W., Washington, DC 20036

J|A|C|S
ARTICLES

Published on Web 06/25/2008

Water Activity Regulates the Q_A^- to Q_B Electron Transfer in Photosynthetic Reaction Centers from *Rhodobacter sphaeroides*

Gerardo Palazzo,*,† Francesco Francia,‡ Antonia Mallardi,§ Mauro Giustini,|| Francesco Lopez,† and Giovanni Venturoli‡

Dipartimento di Chimica and CSGI, Università di Bari, via Orabona 4, I-70126, Bari, Italy, Dipartimento di Biologia and CNISM, Università di Bologna, Italy, Istituto per i Processi Chimico-Fisici, CNR, via Orabona 4, 70126 Bari, Italy, and CSGI and Dipartimento di Chimica, Università "La Sapienza", I-00185 Roma, Italy

Received November 14, 2007; E-mail: palazzo@chimica.uniba.it

Abstract: We report on the effects of water activity and surrounding viscosity on electron transfer reactions taking place within a membrane protein: the reaction center (RC) from the photosynthetic bacterium *Rhodobacter sphaeroides*. We measured the kinetics of charge recombination between the primary photoxidized donor (P^+) and the reduced quinone acceptors. Water activity (a_W) and viscosity (η) have been tuned by changing the concentration of cosolutes (trehalose, sucrose, glucose, and glycerol) and the temperature. The temperature dependence of the rate of charge recombination between the reduced primary quinone, Q_A^-, and P^+ was found to be unaffected by the presence of cosolutes. At variance, the kinetics of charge recombination between the reduced secondary quinone (Q_B^-) and P^+ was found to be severely influenced by the presence of cosolutes and by the temperature. Results collected over a wide η-range (2 orders of magnitude) demonstrate that the rate of $P^+Q_B^-$ recombination is uncorrelated to the solution viscosity. The kinetics of $P^+Q_B^-$ recombination depends on the $P^+Q_A^-Q_B \leftrightarrow P^+Q_AQ_B^-$ equilibrium constant. Accordingly, the dependence of the interquinone electron transfer equilibrium constant on T and a_W has been explained by assuming that the transfer of one electron from Q_A^- to Q_B is associated with the release of about three water molecules by the RC. This implies that the interquinone electron transfer involves at least two RC substates differing in the stoichiometry of interacting water molecules.

Introduction

Proteins are characterized by a complex conformational dynamics. The wide range of internal motions they experience at physiological temperatures originates from rugged energy landscapes, which feature an extremely large number of minima corresponding to different conformational substates, organized in hierarchical tiers.[1–3] This ability of the protein to perform structural fluctuations among many different conformational substates appears to be intimately connected to protein function.[4,5]

The photosynthetic reaction center (RC) from purple bacteria is becoming a paradigmatic system in the study of the relationship between electron transfer processes and protein conformational dynamics. This membrane chromoprotein, following photon absorption by the primary electron donor P (a bacteriochlorophyll dimer), catalyzes a sequential electron tunnelling, which leads in 200 ps to reduction of the primary quinone acceptor Q_A, located 25 Å away from P. From Q_A^- the electron is then delivered to the secondary quinone acceptor Q_B. In the absence of electron donors to P^+, the electron on Q_B^- recombines with the hole on P^+. In Q_B-deprived RCs, recombination of the primary charge-separated state $P^+Q_A^-$ takes place by direct electron tunnelling.[6,7]

A large number of experimental findings indicates that the electric field generated by light-induced charge separation within the RC perturbs substantially the protein, giving rise to conformational changes, which in turn affect electron transfer kinetics. RCs can be trapped at cryogenic temperatures in a dark-adapted and a light-adapted conformation (depending on the illumination and cooling protocols), which drastically differ in the stability of the primary charge-separated state $P^+Q_A^-$.[8,9] Conformational changes within the cytoplasmic domain of RC induced by prolonged illumination have been detected by X-ray diffraction for protein lacking quinone at the Q_B site.[10]

† Università di Bari.
‡ Università di Bologna.
§ CNR.
|| Università "La Sapienza".

(1) Frauenfelder, H.; Sligar, S. G.; Wolynes, P. G. *Science* **1991**, *254*, 1598.
(2) Frauenfelder, H.; Wolynes, P. G. *Phys. Today* **1994**, *47*, 58.
(3) Hofmann, C.; Aartsma, T. J.; Michel, H.; Köhler, J. *Proc. Natl. Acad. Sci. U.S.A.* **2003**, *100*, 15534.
(4) Frauenfelder, H.; McMahon, B. *Proc. Natl. Acad. Sci. U.S.A.* **1998**, *95*, 4795.
(5) Fenimore, P. W.; Frauenfelder, H.; McMahon, B. H.; Parak, F. G. *Proc. Natl. Acad. Sci. U.S.A.* **2002**, *99*, 16047.
(6) Feher, G.; Allen, J. P.; Okamura, M. Y.; Rees, D. C. *Nature* **1989**, *33*, 111.
(7) Gunner, M. R. *Curr. Top. Bioenerg.* **1991**, *16*, 319.
(8) Kleinfeld, D.; Okamura, M. Y.; Feher, G. *Biochemistry* **1984**, *23*, 5780.
(9) McMahon, B. H.; Müller, J. D.; Wraight, C. A.; Nienhaus, G. U. *Biophys. J.* **1998**, *74*, 2567.

 © 2008 American Chemical Society

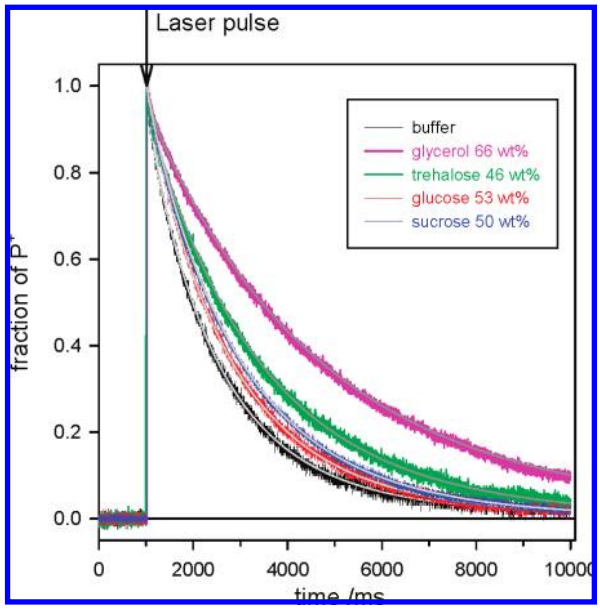

Figure 1. Kinetics of P^+ decay after a laser pulse measured in detergent suspensions of Q_B-reconstituted RCs in the presence of different cosolutes at 20 °C. Also shown are the fits of the data to eq 1 (best-fitting parameters are listed in Table 1).

Studies have focused also on the electron transfer from the photoreduced Q_A^- to the secondary acceptor Q_B.[8,11,12] This electron transfer between Q_A and Q_B is temperature activated, coupled to proton movement, and appears to be conformationally gated.[13] In the crystal structure of RCs cooled to cryogenic temperatures under illumination, that is, trapped in the $P^+Q_AQ_B^-$ state, Q_B was found ~4.5 Å closer to Q_A than in the protein frozen in the dark. Moreover, in this proximal configuration observed in the light, Q_B was flipped by 180° around the isoprenoid chain.[14] A recent X-ray diffraction study,[15] in which the best resolution for the RC structure was attained, confirmed the existence of two different binding positions of Q_B, although no ring flip of the quinone, as compared to the orientation of the proximal state, was observed. The movement of Q_B was originally proposed as the major structural change involved in the conformational gating step.[14] However, the correlation between the large shift in Q_B configuration and the rate-limiting conformational change has been questioned on the basis of subsequent work performed in native and mutated RCs, which suggests more subtle structural rearrangements, possibly involving protein groups or hydrogen-bonding networks, as responsible for the gate.[16–18] The conformational dynamics coupled to Q_A^- to Q_B electron transfer has been recently investigated by us at room temperature by exploiting the incorporation of RCs into trehalose glasses of different trehalose/water ratios.[19,20] Dehydration of RC-containing trehalose matrices causes reversible inhomogeneous inhibition of Q_A^--to-Q_B electron transfer, involving two subpopulations of RCs.[21] In one of such populations ("active"), the electron transfer to Q_B still successfully competes with $P^+Q_A^-$ recombination; in the other one ("inactive"), electron transfer to Q_B after a laser pulse is inhibited dramatically because only recombination of the $P^+Q_A^-$ state is observed. Slight residual water variations modulate the relative fraction of the two populations. The block of Q_A^--to-Q_B electron transfer, following dehydration, was ascribed to a large increase of the energy barriers, which govern the conformational transitions gating electron transfer. Interestingly, while such an effect was qualitatively observed for RCs embedded in several solid matrices, the complete block of the "inactive" to "active"

Table 1. Temperature Dependence of the Parameters of P^+ Decay Determined in the Absence and in the Presence of Different Cosolutes[a]

solution water activity	temperature /°C	λ (s^{-1})[b]	σ (s^{-1})[c]	P_F[d]	η (Pa s)[e]
buffer $a_w = 1.00 \pm 0.02$	29.5	0.81	0.28	0.12	0.0008
	20.5	0.67	0.22	0.06	0.0010
	15.3	0.62	0.22	0.06	0.0011
	9.4	0.58	0.24	0.05	0.0013
	4.5	0.49	0.14	0.08	0.0015
trehalose 46 wt % $a_w =$	35.1	0.72	0.25	0.07	0.014
0.97 ± 0.02	30.0	0.59	0.21	0.02	0.013
	25.7	0.51	0.17	0.04	0.013
	20.5	0.43	0.13	0.04	0.015
	15.3	0.39	0.12	0.03	0.020
	10.3	0.34	0.01	0.04	0.025
glucose 53 wt % $a_w =$	30.0	0.62	0.20	0.03	0.016
0.89 ± 0.02	25.0	0.59	0.19	0.02	0.018
	21.0	0.56	0.16	0.02	0.017
	15.2	0.51	0.16	0.03	0.020
	9.7	0.48	0.14	0.04	0.028
	2.0	0.47	0.18	0.03	0.035
	−3.4	0.43	0.13	0.05	0.042
	−7.6	0.45	0.17	0.05	0.049
sucrose 50 wt % $a_w =$	30.8	0.66	0.22	0.02	0.012
0.96 ± 0.02	25.7	0.57	0.16	0.03	0.014
	20.0	0.51	0.13	0.03	0.017
	15.4	0.46	0.14	0.03	0.021
	10.6	0.42	0.13	0.02	0.027
	6.7	0.39	0.11	0.03	0.032
	2.0	0.38	0.13	0.05	0.040
	0.5	0.38	0.13	0.06	0.043
	−3.2	0.35	0.11	0.08	0.051
	−8	0.35	0.09	0.10	0.066
glycerol 66 wt % $a_w =$	30.6	0.31	0.05	0.1	0.010
0.70 ± 0.02	25.1	0.29	0.08	0.07	0.013
	20.0	0.27	0.07	0.05	0.017
	15.1	0.25	0.08	0.08	0.022
	9.4	0.22	0.06	0.05	0.030
	5.1	0.21	0.06	0.05	0.037
	−0.4	0.18	0.067	0.06	0.051
	−6.7	0.17	0.024	0.05	0.075

[a] Traces have been fitted to eq 1, imposing $k_{AP} = 10\ s^{-1}$. Water activity and viscosity values have been determined experimentally as described in the Experimental Section; a_W is temperature independent (ref 54). [b] Associated 95% confidence interval: ±0.01. [c] Associated 95% confidence interval: ±0.02. [d] Associated 95% confidence interval: ±0.04. [e] Associated 95% confidence interval: ±1 on the last digit.

(10) Katona, G.; Snijder, A.; Gourdon, P.; Andréasson, U.; Hansson, O.; Andréasson, L. E.; Neutze, R. *Nat. Struct. Biol.* **2005**, *12*, 630.
(11) Xu, Q.; Gunner, M. R. *Biochemistry* **2001**, *40*, 3232.
(12) Xu, Q.; Gunner, M. R. *Biochemistry* **2002**, *41*, 2694.
(13) Graige, M. S.; Feher, G.; Okamura, M. Y. *Proc. Natl. Acad. Sci. U.S.A.* **1998**, *95*, 11679.
(14) Stowell, M. H. B.; McPhillips, T. M.; Rees, D. C.; Soltis, S. M.; Abresch, E.; Feher, G. *Science* **1997**, *276*, 812.
(15) Koepke, J.; Krammer, E. M.; Klingen, A. R.; Sebban, P.; Ullmann, G. M.; Friztsch, G. *J. Mol. Biol.* **2007**, *371*, 396.
(16) Kuglstatter, A.; Emler, U.; Michel, H.; Baciou, L.; Fritzsch, G. *Biochemistry* **2001**, *40*, 4253.
(17) Baciou, L.; Michel, H. *Biochemistry* **1995**, *34*, 7967.
(18) Breton, J.; Boullais, C.; Mioskowsky, C.; Sebban, P.; Baciou, L.; Nabedryk, E. *Biochemistry* **2002**, *41*, 12921.
(19) For a review, see: Cordone, L.; Cottone, G.; Giuffrida, S.; Palazzo, G.; Venturoli, G.; Viappiani, C. *Biochim. Biophys. Acta* **2005**, *1749*, 252.
(20) For a review, see: Palazzo, G. *Curr. Opin. Colloid Interface Sci.* **2006**, *11*, 65.
(21) Francia, F.; Palazzo, G.; Mallardi, A.; Cordone, L.; Venturoli, G. *Biophys. J.* **2003**, *85*, 2760.

conformational transition was observed only for trehalose-based glasses.[21–23] This is in line with the remarkable ability of trehalose to hinder protein dynamics[19,24] and stabilize proteins and membranes in the dry state.[25–27] On the other hand, in several organisms trehalose is crucial also for surviving from thermal shock.[28] Under this circumstance, trehalose manifests its bioprotective effectiveness in (liquid) solution at molar concentration, although the precise mechanism of action is still debated. In this respect, a comparative study of the RC functionality in concentrated solutions of molecules used in vivo (bioprotectants) and in vitro (e.g., cryoprotectants) to restrain protein dynamics could give further insights on the energy landscape associated with the electron transfer events. Basically, protein motions can be nonslaved or slaved to solvent motions.[5,29,30] Nonslaved motions are independent of the solvent fluctuations, while slaved protein dynamics depends on the fluctuation rate of the solvent, resulting in a dependence of protein functionality on surrounding viscosity. The functionality of proteins often depends also on the activity of water; hydration can in fact affect the structure and/or the internal dynamics of proteins.[31]

Here, we present a systematic study on the effect of viscosity and water activity on the recombination kinetics of the $P^+Q_AQ_B^-$ state induced by a laser actinic pulse on reaction centers purified from the purple bacteria *Rhodobacter* (*Rb.*) *sphaeroides*. These environmental parameters have been tuned by changing the concentration of cosolutes and the temperature. We used as cosolutes two disaccharides (trehalose and sucrose) and the monosaccharide glucose because of their physiological relevance and glycerol because it is widely used as cryoprotectant for in vitro studies.

Experimental Section

N,*N*-Dimethyldodecylamine-*N*-oxide (LDAO) was purchased from Fluka as 30% aqueous solution. Glucose, sucrose, ubiquinone-Q10, and glycerol were from Sigma-Aldrich. Dihydrate trehalose was from Hayashibara Shoij Inc. (Okayama, Japan).

Samples were prepared first by dissolving suitable amounts of cosolutes in water (to dissolve sugars, the mixture was first warmed and subsequently cooled to room temperature), and then by adding a few microliters of concentrated buffer and RCs to a final concentration of 10 mM Tris-HCl pH = 8.0, 0.025 wt/vol % LDAO, 2.5 μM RC. The cosolute concentration was evaluated by weight and reported as weight percent (wt %), that is, (weight of cosolute)/(overall sample weight) %.

RCs from *Rhodobacter* (*Rb.*) *sphaeroides* were isolated and purified according to Gray et al.[32] In all preparations, the ratio of the absorption at 280 and 800 nm was between 1.2 and 1.3. This isolation procedure gives RCs with a Q_B content/activity of about 60%. To reconstitute secondary quinone acceptor, the purified RC was loaded on a column of DE-52 (Wathman) previously equilibrated with ubiquinone-10 containing buffer. The low solubility of ubiquinone-10 in aqueous buffer was overcome by adding the quinone to the 30% LDAO stock solution used for preparing buffer. The RCs were extensively washed with the same buffer, eluted with 400 mM NaCl, and dialyzed overnight (to remove the salt). Q_B activity of the reconstituted samples was typically higher than 95%.

The kinetics of charge recombination were measured spectrophotometrically by following the decay of the oxidized primary donor (P^+) generated by a laser pulse (frequency doubled Nd:YAG, Quanta System, Handy 710; 7 ns pulse width; 200 mJ pulse energy). The rapid absorbance changes were monitored by using one of two kinetic spectrophotometers of local design described in ref 23. The kinetics of charge recombination were monitored either at 605 or at 860 nm (depending on the apparatus). The cell holder was thermostatted using a cryothermostat (Haake F3K); the temperature of the sample was monitored by a Pt-100 resistance thermometer (Degussa GR 2105) with a tolerance of 0.3 °C, immersed directly into the sample. The survival probability, $I(t)$, of P^+ was evaluated as the absorbance change kinetics normalized to the absorbance change at time $t = 0$ ($I(t) = \Delta\mathrm{Abs}(t)/\Delta\mathrm{Abs}(0)$). An adequate and physically meaningful function fitting the survival probability $I(t)$ of P^+ (i.e., the decay of the fraction of RC in the charge-separated state) is:[33]

$$I(t) = P_F \exp(-k_{AP}t) + (1 - P_F) \exp\left(-\lambda t + \frac{\sigma^2}{2}t^2\right) \qquad (1)$$

where the term $P_F \exp(-k_{AP}t)$ accounts for the fraction (P_F) of RCs undergoing a fast $P^+Q_A^-$ recombination, and the truncated cumulant expansion describes a continuous distribution of decay rates due to the slow $P^+Q_AQ_B^-$ recombination. As described in the Supporting Information, λ is the average rate constant and σ^2 is the variance of the rate distribution.

Viscosity measurements as a function of the temperature (concentrated samples) were performed on a Physica UDS 200 rheometer using a cone-plate geometry (25 mm, 2°); the viscosity was evaluated from the slope of shear stress against shear rate plot in continuous shear measurements (all of the samples obey the Newtonian behavior). Viscosity measurements at 23 °C (dilute samples) have been carried out using a vibrational viscosimeter (SV-10, A&D Co. Ltd., Japan) and were corrected for the density.

The activity of water (a_W) was measured for all of the samples at 23 °C using a water activity meter (PA_wkit, Decagon Devices Inc.) previously calibrated with suitable standards (tolerance ± 0.02 a_W).

Results and Discussion

Features of the Charge Recombination Kinetics. Figure 1 compares the kinetics of P^+ recombination following a light flash recorded in Q_B-reconstituted RCs solubilized in buffer and in concentrated cosolute/buffer solutions. It is clear that the presence of different cosolutes (66 wt % glycerol, 46 wt % trehalose, 50 wt % sucrose, and 53 wt % glucose) strongly affects the decay of the protein charge-separated state.

When isolated RCs are activated by a flash of light, the state $P^+Q_A^-Q_B$ is formed in less than 200 ps. Subsequent electron transfer events can be suitably described by the following scheme:[34]

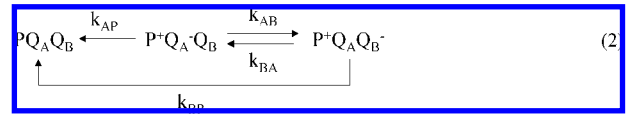

(2

Under physiological conditions, $k_{AP} \approx 10\ s^{-1}$, $k_{AB} \approx 6 \times 10^3\ s^{-1}$, and $k_{BA} \approx 4.5 \times 10^2\ s^{-1}$; the contribution of direct electron

(22) Francia, F.; Giachini, L.; Palazzo, G.; Mallardi, A.; Boscherini, F.; Venturoli, G. *Bioelectrochemistry* **2004**, *63*, 73.
(23) Mallardi, A.; Giustini, M.; Lopez, F.; Dezi, M.; Venturoli, G.; Palazzo, G. *J. Phys. Chem. B* **2007**, *111*, 3304.
(24) Cordone, L.; Ferrand, M.; Vitrano, E.; Zaccai, G. *Biophys. J.* **1999**, *76*, 1043.
(25) Leslie, S. B.; Israeli, E.; Lighthaert, B.; Crowe, J. H.; Crowe, L. M. *Appl. Environ. Microbiol.* **1995**, *91*, 3592–3597.
(26) Crowe, L. M.; Reid, D. S.; Crowe, J. H. *Biophys. J.* **1996**, *71*, 2087–2093.
(27) Crowe, J. H. In *Molecular Aspects of the Stress Response: Chaperones, Membranes and Networks*; Csermely, P., Vìgh, L., Eds.; Springer Science: New York, 2007; Chapter 13, p 143.
(28) Singer, M. A.; Lindquist, S. *Trends Biotechnol.* **1998**, *16*, 460.
(29) Frauenfelder, H.; Fenimore, P. W.; McMahon, B. H. *Biophys. Chem.* **2002**, *98*, 35.
(30) Frauenfelder, H.; Fenimore, C. G.; McMahon, P. W. *Proc. Natl. Acad. Sci. U.S.A.* **2006**, *103*, 15469.
(31) Rand, R. P. *Philos. Trans. R. Soc. London, Ser. B* **2004**, *359*, 1277.

transfer from Q_B^- to P^+, characterized by the rate constant k_{BP}, is negligible in native RCs in room temperature buffer.[35] For the sake of simplicity, we will assume in the following $k_{BP} = 0$ under all of the experimental conditions tested. Calculations that explicitly take into account the direct recombination from Q_B^- are reported in the Supporting Information and discussed below. For $k_{BP} = 0$, charge recombination of the $P^+Q_AQ_B^-$ state occurs by thermal repopulation of $P^+Q_A^-Q_B$ state with an observable overall rate constant λ, which is determined by the value of k_{AP} and the fraction of RCs undergoing $P^+Q_A^-Q_B$ charge recombination according to:[34]

$$\lambda = \frac{k_{AP}}{1 + L_{AB}}; \qquad L_{AB} = \frac{[P^+Q_AQ_B^-]}{[P^+Q_A^-Q_B]} \tag{3}$$

Recombination of the $P^+Q_AQ_B^-$ state will follow strictly a monoexponential decay with rate constant λ only if the Q_B site is fully occupied and if the exchange kinetics of the quinone molecule at the Q_B site with quinone molecules present in the detergent phase can be neglected. Quinone exchange, which occurs rapidly on the time scale of the processes of reaction 2, gives rise to a recombination kinetics distributed over a spectrum of rate constants (see the Supporting Information). As discussed in the Supporting Information, λ is influenced by the quinone exchange at the Q_B site, and for the RCs reconstituted with excess ubiquinone we expect only a narrow spreading of the λ-values; for RC in buffer at room temperature, typical values are between 0.6 and 0.7 s^{-1} depending on the efficiency of the reconstitution procedure.

In the absence of the secondary acceptor Q_B, or when Q_A^- to Q_B electron transfer is blocked, direct recombination of the $P^+Q_A^-$ state occurs so that P^+ decays faster with rate constant k_{AP}:

$$PQ_A \underset{k_{AP}}{\overset{h\nu}{\rightleftharpoons}} P^+Q_A^- \tag{4}$$

As a consequence, the decay of P^+ following a short photoexcitation includes in general two kinetic components, a fast and a slow one, ascribed to RC subpopulations that undergo $P^+Q_A^-$ and $P^+Q_B^-$ recombination, respectively. The relative contributions of the two components depend on the fraction of RC in which the final electron transfer from Q_A^- to Q_B cannot take place.

All of the charge recombination kinetics collected in the present work have been satisfactorily accounted for by eq 1 (representative fits are shown in Figure 1). When fitting the traces of Q_B-reconstituted RCs, we fixed the rate constant of the fast phase to 10 s^{-1}, a typical value for $P^+Q_A^-$ recombination. This was done to avoid effects of strong parameter correlation and in view of the low amplitude of the fast kinetic component.

The P^+ decays were measured in buffer and in the four concentrated glycerol and sugars solutions at different temperatures. The best-fit parameters obtained from the analysis described above are listed in Table 1. In all of the cases, the fraction of fast phase, P_F, and the width of the distribution of slow rates are scarcely affected by the temperature. On the contrary, the average rate λ of $P^+Q_AQ_B^-$ charge recombination increases with temperature and depends markedly on the solution composition.

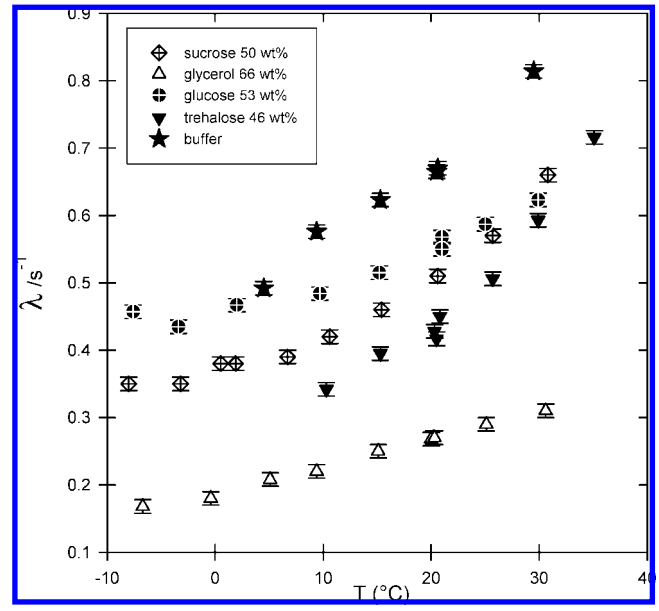

Figure 2. Temperature dependence of the average rate constant (λ) of $P^+Q_AQ_B^-$ recombination determined in detergent RC suspensions in the absence and in the presence of different cosolutes. Values of λ have been evaluated by fitting charge recombination kinetics to eq 1 (other best-fitting parameters are listed in Table 1).

As shown in Figure 2, for all of the temperatures the higher λ-values are observed in the absence of cosolvents (i.e., in 10 mM Tris, 0.025% LDAO) and the lower λ-values are found in concentrated glycerol solutions. The rate of $P^+Q_AQ_B^-$ charge recombination observed for sugar solutions lies between these extremes according to the order buffer > glucose > sucrose > trehalose > glycerol. These effects are fully reversible: the systems do not show thermal hysteresis, and removal of cosolutes by size-exclusion chromatography restores the behavior found for RCs in buffer.

$P^+Q_A^-$ Charge Recombination Kinetics. To unravel the various effects of the environment on the $P^+Q_AQ_B^-$ charge recombination, we have also determined, for each solution, the temperature dependence of the rate of $P^+Q_A^-$ charge recombination. This was done by analyzing the P^+ decay measured in purified RCs, which were not loaded with excess exogenous quinone. Following purification, a large fraction (more than 40%) of protein is deprived of quinone at the Q_B site, as judged from the large relative amplitude of the fast kinetic component of P^+ decay. Under these conditions, the initial part of the experimental decay is dominated by the fast recombination from Q_A^-, and fitting the initial part ($t < 1$ s) of the P^+ decay according to eq 1 furnishes safe values of the rate constant k_{AP}. As shown in Figure 3, the rate constant of charge recombination from Q_A^- decreases with the temperature under all of the conditions tested. Such an unusual behavior already documented for RCs in buffers and in glycerol–buffer mixtures[36] is shared also by the RCs in sugar–buffers mixtures. Around room

(32) Gray, K. A.; Wachtveitl, J.; Breton, J.; Oestherhelt, D. *EMBO J.* **1990**, *9*, 2061.
(33) Ambrosone, L.; Mallardi, A.; Palazzo, G.; Venturoli, G. *Phys. Chem. Chem. Phys.* **2002**, *4*, 3071.
(34) Shinkarev, V. P.; Wraight, C. A. In *The Photosynthetic Reaction Center*; Deisenhofer, J., Norris, J. R., Eds.; Academic Press: New York, 1993; Vol. 1, p 193; and references therein.
(35) Kleinfeld, D.; Okamura, M. Y.; Feher, G. *Biochim. Biophys. Acta* **1984**, *766*, 126–140.
(36) See refs in: Krasilnikov, P. M.; Mamonov, P. A.; Knox, P. P.; Paschenko, V. Z.; Rubin, A. B. *Biochim. Biophys. Acta* **2007**, *1767*, 541.

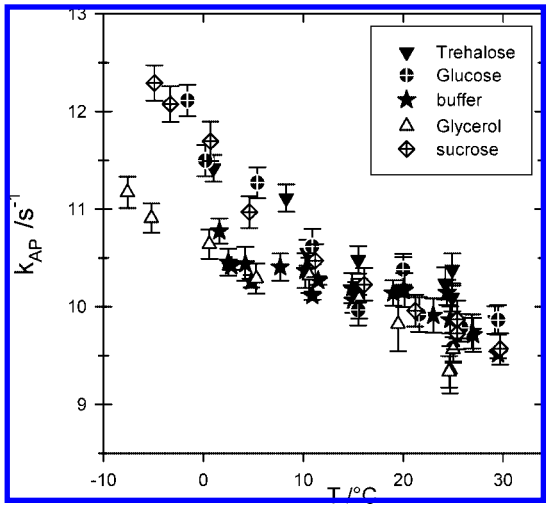

Figure 3. Temperature dependence of the rate constant k_{AP} of $P^+Q_A^-$ recombination in the absence and in the presence of different cosolutes. Measurements were performed under the same conditions as in Figure 2, except that purified RCs were not reconstituted in Q_B activity (see text for details).

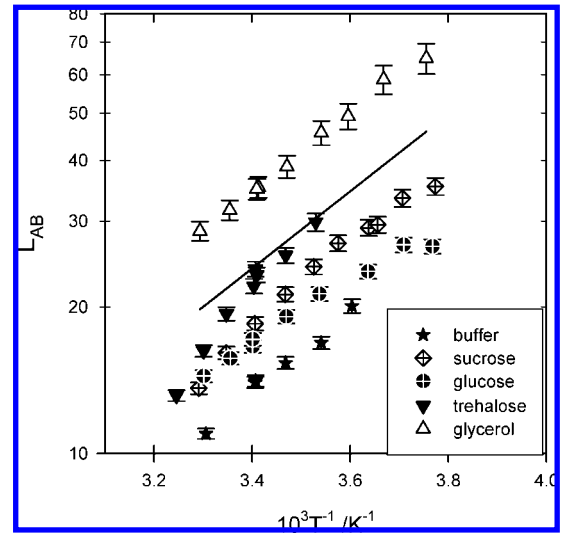

Figure 4. van't Hoff plot for the interquinone electron transfer equilibrium constant (L_{AB}) determined from the data of Figures 2 and 3 assuming saturation of the Q_B-site (eq 5). The straight line represents the temperature dependence of L_{AB} as determined for RCs embedded in phosphatidylcholine vesicles, corresponding to $\Delta H_{AB}^\circ = -15.2$ kJ mol^{-1} (from ref 39).

temperature, the nature of cosolutes does not influence the k_{AP}, and only below 10 °C do kinetics measured in the sugars solutions differ slightly from those measured in buffer and glycerol, k_{AP} being higher in the presence of sugars.

What really matters for the purpose of the present analysis is that k_{AP} is a decreasing function of the temperature, so that (according to eq 3) the increase in the rate of $P^+Q_AQ_B^-$ charge recombination observed upon increasing T (see Figure 2) can be accounted for only by assuming a decrease in the apparent equilibrium constant L_{AB} for the interquinone electron transfer.

***T*-Dependence of $P^+Q_A^-Q_B \leftrightarrow P^+Q_AQ_B^-$ Equilibrium.** L_{AB} can be evaluated using the data of Figures 2 and 3 as:

$$L_{AB} = \frac{k_{AP}}{\lambda} - 1 \qquad (5)$$

With L_{AB} an (apparent) equilibrium constant, its T-dependence is better analyzed in a van't Hoff plot (Figure 4). Within the limited temperature range of our measurements, the logarithmic plots of L_{AB} versus $1/T$ are well described by linear relationships. Interestingly, the slopes of the van't Hoff plots are mutually close for all of the systems. The thermodynamics of the interquinone electron transfer is reasonably well understood; the $Q_A^-Q_B \rightarrow Q_AQ_B^-$ electron transfer is known to be exothermic with an enthalpy change (ΔH_{AB}°) of about -15 kJ mol^{-1} and an entropy change of about -25 J·K^{-1} mol^{-1}.[37–39] For comparison, the temperature dependence of L_{AB} determined in lipid vesicles[39] is also shown in Figure 4.

Because in the van't Hoff representation, the slope corresponds to $-\Delta H_{AB}^\circ/R$, Figure 4 indicates that such a quantity is scarcely affected by the presence of cosolutes, the notable exception being the trehalose where the slope seems to be 40% larger at high temperature.

Viscosity Effect. When examining the effect of solutes on the protein functionality, it is important to consider all of the environmental properties through which cosolutes can affect the protein structure and dynamics. The solution viscosity η and the water activity a_w, in particular, are both known to affect the functionality of several proteins. Strictly, viscosity should not affect a pure thermodynamic property such as an equilibrium constant. However, L_{AB} is evaluated according to eq 5 from the ratio between two rate constants. Reaction 2, underlying eqs 3 and 5, is only a simplified one, and evidence suggests that the $P^+Q_A^-Q_B \leftrightarrow P^+Q_AQ_B^-$ electron transfer is associated with one or more conformational transitions of the protein. If one of these conformational changes is rate determining for the back electron transfer, it is conceivable that λ and thus the apparent L_{AB} could be affected by the viscosity of the surrounding.

Within the framework of Kramer theory for unimolecular processes, the rate constant of the interconversion, κ, is inversely proportional to a generalized friction coefficient ζ (i.e., $\kappa \propto \zeta^{-1}$).[40,41] In some cases, the interpretation of ζ has been straightforward: for geminate rebinding of CO to myoglobin, ζ has been essentially identified with the bulk viscosity η of the medium;[42,43] the same rationale has been found adequate to describe the effects of cosolvents on the rate of $P^+Q_A^-$ charge recombination in RCs from *Rps. virids*.[44] For these systems and processes, it was concluded that the surface diffusive motions are strongly coupled with the reactive modes of the protein, the former being slowed down by a mere solvent viscosity effect.

The viscosity of sugars and glycerol solutions used in the present study is more than 1 order of magnitude higher than that of buffer. Therefore, the similarity between k_{AP}-values measured in the presence and in the absence of cosolutes (Figure 3) indicates that for RCs from *Rb. sphaeroides* the rate of charge

(37) Mancino, L. J.; Dean, D. P.; Blankenship, R. E. *Biochim. Biophys. Acta* **1984**, *764*, 46.
(38) Mallardi, A.; Palazzo, G.; Venturoli, G. *J. Phys. Chem. B* **1997**, *101*, 7850.
(39) Palazzo, G.; Mallardi, A.; Giustini, M.; Berti, D.; Venturoli, G. *Biophys. J.* **2000**, *79*, 1171.
(40) Gavish, B. *Phys. Rev. Lett.* **1980**, *44*, 1160.
(41) Billing, G. D.; Mikkelsen, K. V. Energetic aspects of solvent effects on solutes. In *Introduction to Molecular Dynamics and Chemical Kinetics*; John Wiley & Sons, Inc.: New York, 1996; pp 98−163.
(42) Ansari, A.; Jones, C. M.; Henry, E. R.; Hofrichter, J.; Eaton, W. A. *Science* **1992**, *256*, 1796.
(43) Kleinert, T.; Doster, W.; Leyser, H.; Petry, W.; Schwartz, V.; Settles, M. *Biochemistry* **1998**, *37*, 717.
(44) Shopes, R. J.; Wraight, C. A. *Biochim. Biophys. Acta* **1987**, *893*, 409.

Table 2. Kinetic Parameters of $P^+Q_AQ_B^-$ Recombination Determined from P^+ Decays Measured at $T = 23$ °C as a Function of Trehalose and Glycerol Concentration[a]

concentration (wt %)	λ (s^{-1})[b]	σ (s^{-1})[c]	P_F[d]	η (Pa s)[e]	a_w[f]
		Trehalose			
14.5	0.51	0.12	0.04	0.0019	0.99
22.6	0.50	0.052	0.05	0.0024	0.99
28.0	0.49	0.155	0.04	0.0036	0.98
36.2	0.48	0.143	0.05	0.0060	0.98
48.0	0.45	0.160	0.06	0.014	0.97
90.0 (wet glass)[g]	0.43	0.18 ± 0.07	0.06	∞	0.39[g]
95.4 (dry glass)[g]	0.41 ± 0.04	0.24 ± 0.05	0.46	∞	0.20[g]
		Glycerol			
11.1	0.56	0.07	0.10	0.0016	0.98
27.3	0.51	0.14	0.09	0.0025	0.94
33.5	0.50	0.16	0.08	0.0032	0.92
38.6	0.47	0.17	0.05	0.0039	0.89
44.5	0.40	0.06	0.08	0.0052	0.86
50.0	0.41	0.09	0.04	0.0068	0.82
58.3	0.32	0.06	0.08	0.0107	0.76
63.7	0.26	0.06	0.12	0.0148	0.72
68.1	0.21	0.07	0.23	0.0197	0.68

[a] Traces have been fitted to eq 1, imposing $k_{AP} = 10\ s^{-1}$. Unless otherwise stated (see footnote g), water activity and viscosity values have been determined experimentally as described in the Experimental Section. [b] Associated 95% confidence intervals (unless otherwise stated): ± 0.01. [c] Associated 95% confidence intervals (unless otherwise stated): ±0.02. [d] Associated 95% confidence intervals (unless otherwise stated): ±0.04. [e] Associated 95% confidence intervals: ±1 on the last digit. [f] Associated 95% confidence intervals: ±0.02. [g] For trehalose glasses, kinetic parameters are from ref 21, and the corresponding values of a_W were calculated according to ref 54.

recombination from Q_A^- is uncorrelated to the viscosity of the surroundings (at variance, a strong dependence of k_{AP} on η has been reported for RCs purified from *Rps. viridis*).[44] In passing, this indicates that the mechanism of $P^+Q_A^-$ recombination, and/or the RC dynamics coupled to this reaction, are substantially different in RCs from *Rb. sphaeroides* and *Rps. viridis*, despite their structural similarity.

The case of $P^+Q_AQ_B^-$ charge recombination taking place in *Rb. sphaeroides* RCs is more complicated because the rate constant λ in buffer is markedly different from the values observed in the presence of cosolutes (Figure 2). To gain insight on these effects, we have tuned, at constant temperature, the viscosity of the system by varying the concentration of glycerol or trehalose. The P^+ decays recorded at 23 °C have been fitted to eq 1. Best-fitting parameters are listed in Table 2. In the case of both glycerol and trehalose, the average rate constant for the $P^+Q_AQ_B^-$ recombination was found to decrease continuously upon increasing the concentration of the cosolutes. To test if this behavior can be accounted for by the parallel increase in the solution viscosity, in Figure 5 we have plotted, as a function of η, the λ-values obtained for all of the cosolutes along isopleths (Table 1) and isotherms (Table 2). It is clear that there is not a unique dependence of the rate of charge recombination on the viscosity; instead different viscogens behave differently. This is particularly evident when comparing the behavior of sugars with that of glycerol solutions. As discussed above, an increase in temperature results in an increase in λ, and because viscosity decreases with temperature we observe for the isopleths of Figure 5 a decline in the rate of charge recombination when plotted against the viscosity. However, such a decrease does not imply necessarily a genuine viscosity dependence. Indeed, we observe the same λ-value, say $\sim$0.5 s^{-1}, over a range of viscosity of about 1 order of magnitude, at the same temperature.

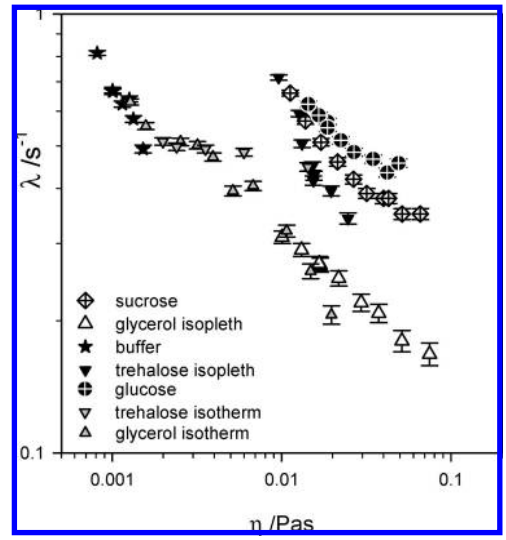

Figure 5. Log−log plot of the rate of $P^+Q_AQ_B^-$ recombination against the solution viscosity. All of the data of Tables 1 and 2 are shown. Symbols for measurements at constant cosolute concentration and variable temperature (isopleths) are as in Figure 2. Gray symbols denote measurements performed at 23 °C and variable cosolute concentration (isotherms).

Consistently, at a viscosity of, for example, 0.02 Pa s, we observe a spread of rate constants from $\lambda \approx 0.2\ s^{-1}$ in the glycerol solution to $\lambda \approx 0.6\ s^{-1}$ in the glucose and trehalose solutions. From these observations, we infer that the influence of viscosity on the rate of $P^+Q_AQ_B^-$ recombination and thus on L_{AB} (according to eq 5) is negligible. Because the structural relaxation time of the solution is proportional to its viscosity through the Maxwell relation $\tau = \eta/G_\infty$, the rate of $P^+Q_AQ_B^-$ charge recombination is independent from solvent relaxation (the high frequency shear modulus G_∞ is almost independent from composition and temperature).[45] In other words, protein dynamics involved in this electron transfer is nonslaved to solvent motions.

Influence of Water Activity on L_{AB}. At the high cosolute concentrations of the present study, also the activity of the solvent water is heavily influenced, and this is known to have strong effects on the conformational transitions of several proteins.[31,46,47] We can understand how an osmotic stress could tune the RC functionality on the basis of the following simplified arguments (for a general treatment, leading to the same conclusions, see ref 46).

Assuming that the reagents and the products (say $P^+Q_A^-Q_B$ and $P^+Q_AQ_B^-$) differ in the number of water (W) and solute (S) molecules that interact with the protein, we can describe the $P^+Q_A^-Q_B \rightarrow P^+Q_AQ_B^-$ electron transfer according to the reaction:

$$P^+Q_A^-Q_B + \Delta N_W H_2O + \Delta N_S \text{solute} \rightarrow P^+Q_AQ_B^- \qquad (6)$$

where ΔN_W and ΔN_S denote the difference in water and solute molecules interacting with the protein in the two states (these quantities can be positive, null, or negative).

(45) In the T-range explored here, G_∞ is almost T-independent, and it is expected to vary only slightly with solution composition (e.g., at room temperature, $G_\infty \sim 1 \times 10^8$ Pa for 75 wt % glycerol/water and $G_\infty \sim 5 \times 10^8$ Pa for 90 wt % sucrose/water); see ref 43.

(46) Ebel, C. In *Protein Interactions*; Schuck, P., Ed.; Springer: New York, 2007; Chapter 9, p 255; and refs therein.

(47) Parsegian, V. A.; Rand, R. P.; Racu, D. C. *Methods Enzymol.* **1995**, *259*, 43.

Accordingly, the equilibrium constant for reaction 6 is

$$K_{eq} = \frac{[P^+Q_A Q_B^-]}{[P^+Q_A^- Q_B] a_W^{\Delta N_W} a_S^{\Delta N_S}} = L_{AB} \frac{1}{a_W^{\Delta N_W} a_S^{\Delta N_S}} \quad (7)$$

and we can write

$$\ln(L_{AB}) = \ln(K_{eq}) + \Delta N_W \ln(a_W) + \Delta N_S \ln(a_S) \quad (8)$$

Equation 8 can be derived with respect to $\ln(a_W)$ bearing in mind that water and solute interacting with the protein are in equilibrium with the bulk solution (far apart from the protein surface) so that their chemical potentials on the protein surface must obey the Gibbs−Duhem equation in the bulk ($n_W\, d\mu_W + n_S\, d\mu_S = n_W\, d\ln(a_W) + n_S\, d\ln(a_S) = 0$); thus:

$$\frac{d\ln(L_{AB})}{d\ln(a_W)} = \Delta N_W - \Delta N_S \frac{n_W}{n_S} = \Delta N_{exc,W} \quad (9)$$

where n_W/n_S is the ratio between water and solute molecules in the bulk. The term $\Delta N_S n_W/n_S$ is the difference in hydration water between the two RC states one expects if the bulk composition holds at the interface of the protein; that is, it is the excess difference in water associated with the protein. $\Delta N_{exc,W}$ can also be expressed in terms of the partition coefficient, $K_P \equiv (N_S/N_W)/(n_S/n_W)$, of the solute between the bulk and the protein surface,[47] obtaining

$$\Delta N_{exc,W} = \Delta N_W (1 - K_P) \quad (10)$$

and thus it is independent from the solute concentration. According to eq 9, in the case of $\Delta N_{exc,W} \neq 0$, we expect the logarithm of L_{AB} to be linearly dependent on the logarithm of water activity with a slope equal to $\Delta N_{exc,W}$.[47,48] The constraint of Gibbs−Duhem relation dictates that any variation in water activity is paralleled by a variation in solute activity, that is, $d\ln(a_W) = -(n_S/n_W)\, d\ln(a_S)$. This results in:[47,48]

$$\frac{d\ln(L_{AB})}{d\ln(a_S)} = -\Delta N_{exc,W} \frac{n_S}{n_W} \quad (11)$$

Because $\ln(a_S)$ is strongly dependent on n_S/n_W, eq 11 predicts a strongly nonlinear dependence of ln L_{AB} on ln[S]. On the contrary, in the case of direct solute–protein interactions (e.g., binding) that alter the interquinone electron transfer, one expects a linear relation between ln L_{AB} and ln[S].[49]

To explore the influence of a_W on the $P^+Q_AQ_B^-$ charge recombination, we focused our analysis on the isothermal data of Table 2. Note also that experimentally a_W can be tuned only to a limited extent in solutions of sugars because concentrated solutions (wt % > 50) tend to be metastable and are cumbersome to prepare; at variance glycerol and water can be easily mixed at any ratio at room temperature so that a wide range of a_W (1−0.68) was accessible only with glycerol.

The L_{AB} values determined at 23 °C at different glycerol and trehalose concentrations fully obey the predictions of eqs 9 and 11. In Figure 6A, the logarithm of the equilibrium constant for the interquinone electron transfer is shown to be linearly dependent on $\ln(a_W)$, as predicted by eq 9. The L_{AB} values have been normalized to the value measured in buffer, $L_{AB,[S]=0}$, to take into account small (∼10%) variations in λ most likely due to slight differences in the efficacy of quinone reconstitution procedure in different RC preparations. Glycerol data are nicely fitted to eq 9 furnishing a value of $\Delta N_{exc,W} = -3.0 \pm 0.3$. The data collected in the presence of trehalose follow eq 9 as well, and linear regression of the data gives $\Delta N_{exc,W} = -6.5 \pm 1.5$. Interestingly, the L_{AB} value determined in 50 wt % sucrose follows the trend observed in trehalose, while the L_{AB} value determined in 53 wt % glucose follows the trend observed in glycerol. In Figure 6B, the same L_{AB} values are plotted as a function of the logarithm of cosolute concentration, a quantity expected to be proportional to the solute activity (at least at low concentration). It is evident that the $\ln(L_{AB})$ versus ln[S] plot is strongly nonlinear as predicted by eq 11, and this rules out the presence of strong osmolyte–RC interactions (ligand-binding). A quantitative comparison with the behavior expected

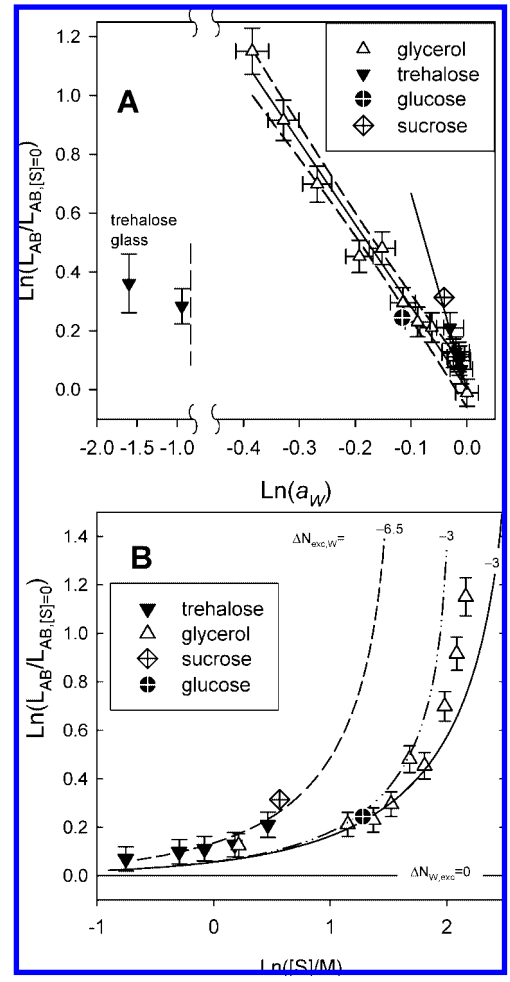

Figure 6. Equilibrium constant for interquinone electron transfer at constant temperature (23 °C). (A) Apparent interquinone electron transfer constant L_{AB} (normalized to the value measured in buffer $L_{AB,\,[S]=0}$) in the presence of glycerol or trehalose as a function of the water activity. The solid lines are the best fit of the data to eq 9 (glycerol, $\Delta N_{exc,W} = -3.0 \pm 0.3$; trehalose, $\Delta N_{exc,W} = -6.5 \pm 1.5$); dashed lines represent the 95% confidence intervals for glycerol regression. Also shown are two data from ref 20 obtained in trehalose glasses. The glucose and sucrose data at 23 °C have been calculated by interpolation of the data in Table 1. (B) Log−log plot of $L_{AB}/L_{AB,[S]=0}$ versus the cosolute concentration; lines represent the prediction according to eq 13. Parameters: $\upsilon_W = 18$ cm^3 mol^{-1}; for glycerol (–) $\Delta N_{exc,W} = -3$ and $\upsilon_S = 73$ cm^3 mol^{-1}; for trehalose and sucrose (– – –) $\Delta N_{exc,W} = -6.5$ and $\upsilon_S = 211$ cm^3 mol^{-1}; for glucose (– • • – • • –) $\Delta N_{exc,W} = -3$ and $\upsilon_S = 116$ cm^3 mol^{-1}.

(48) Parsegian, V. A.; Rand, R. P.; Racu, D. C. *Proc. Natl. Acad. Sci. U.S.A.* **2000**, *97*, 3987.

(49) The case of solute binding that influences the electron transfer corresponds to reaction 6 with $\Delta N_W = 0$ and thus $\Delta N_{W,exc} = -\Delta N_S n_W/n_S$. Under this circumstance, the derivative in eq 11 becomes constant and equal to ΔN_S, the number of solute molecules bound or released upon electron transfer.

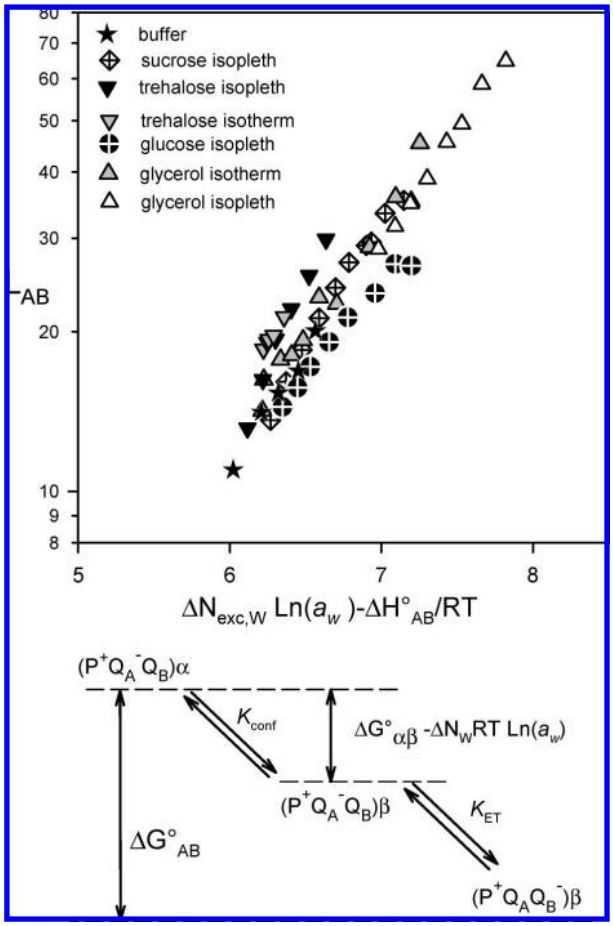

Figure 7. Upper panel: Dependence of ln L_{AB} upon $F(T, a_W)$ (defined in eq 16). $F(T, a_W)$ values have been evaluated assuming $\Delta H_{AB}^{\circ} = -15$ kJ mol^{-1} for all of the samples of Tables 1 and 2 and $\Delta N_{exc,W} = -3$ for data obtained in glycerol and glucose solutions and $\Delta N_{exc,W} = -6.5$ for data obtained in trehalose and sucrose solutions. Symbols are as in Figures 4 and 5. Lower panel: Energy diagram for the conformational gating of the electron transfer described by the reaction 17. The free energy level of the intermediate $(P^+Q_A^-Q_B)\beta$ state formed by the release of $-\Delta N_W$ water molecules decreases by an amount $\Delta N_W RT$ for a unitary decrease in ln(a_W).

according to eq 11 can be done taking into account the relationship between n_S/n_W and the solute molar concentration [S]:[50]

$$\frac{n_S}{n_W} = \frac{[S]}{\frac{1}{v_W}(1 - [S]v_S)} = \frac{v_W e^{\ln[S]}}{1 - v_S e^{\ln[S]}} \qquad (12)$$

where v_W and v_S denote the molar volume of water and solute, respectively. Assuming ln(a_S) ≈ ln[S], eq 11 can be integrated, obtaining

$$\ln\left(\frac{L_{AB}}{L_{AB,[S]=0}}\right) = \Delta N_{exc,W} v_W \frac{\ln\left(1 - v_S e^{\ln[S]}\right)}{v_S} \qquad (13)$$

In Figure 6B, the predictions of eq 13 are compared to the experimental results assuming for trehalose and sucrose $\Delta N_{exc,W} = -6.5$ and for glycerol and glucose $\Delta N_{exc,W} = -3.0$ as inferred from Figure 6A. Actually the curves in Figure 6B are true predictions without any adjustable parameter. Equation 13 well describes the experimental data up to a solute concentration of 6 M (accessible only by using glycerol); at higher cosolute concentration the agreement is poorer, most likely because the approximation ln(a_S) ≈ ln[S] is no more acceptable. The data representation of Figure 6B emphasizes the different behavior observed for disaccharides and for smaller osmolytes (viz. glycerol and glucose). In principle, $\Delta N_{exc,W}$ depends on the cosolute nature being related to the partition coefficient of the solute between the bulk and the protein surface (see eq 10). For molecules of akin structures (polyols in the present case), the preferential exclusion from (or binding to) the protein surface is expected to depend mainly on their relative size.[46,47] Accordingly, the drop in $\Delta N_{exc,W}$ observed passing from disaccharides to glucose reflects the reduction in the molecular volume. However, further reduction in osmolyte size (from glucose to glycerol) does not affect the $\Delta N_{exc,W}$ values. This is expected when the water involved in reaction 6 is secluded within cavities, which are totally impermeable to osmolyte molecules (i.e., $\Delta N_S = 0$). In this case, the protein scaffolding acts as a semipermeable membrane, and water is extracted or adsorbed from the protein by the solution osmotic pressure. Under this circumstance, $\Delta N_{exc,W}$ is equal to the number of water molecules expelled or adsorbed during reaction 6 ($\Delta N_{exc,W} = \Delta N_W$).[48,51]

Relevance of Direct $P^+Q_AQ_B^-$ Recombination. The charge recombination through the $P^+Q_A^-Q_B$ state is the prevalent route of Q_B^- and P^+ recombination in purified RCs in buffer at room temperature. Indeed, it was firmly established that under these conditions such a path is kinetically dominant over the direct electron transfer from Q_B^-.[35] The rate constant (k_{BP}) of direct charge recombination between Q_B^- and P^+ was estimated in experiments performed with RCs reconstituted with low potential quinones at the Q_A site. In these cofactor-modified RCs, the thermal repopulation of $P^+Q_A^-Q_B$ state is disadvantaged, thus allowing the measurement of the direct recombination rate constant k_{BP}. For RCs in buffer at 293 K, a k_{BP} value of 0.12 s^{-1} was measured,[52] and the addition of glycerol at a concentration of 65 wt % does not change this estimate.[53] These values of direct recombination rate are comparable to the λ-values observed in the present work at high osmolyte content. This suggests that a better estimate of the apparent equilibrium constant L_{AB} should include the contribution of the direct route for $P^+Q_AQ_B^-$ recombination.

We have therefore evaluated the equilibrium constant for the $P^+Q_A^-Q_B \leftrightarrow P^+Q_AQ_B^-$ electron transfer taking into account the "direct recombination" as detailed in the Supporting Information. This contribution turned out to become important at low water activity (small λ values), and this resulted in a systematic increase in the $\Delta N_{W,exc}$ evaluated according to eq 11 (e.g., $\Delta N_{W,exc} = -4.3 \pm 0.7$ for glycerol). The overall dependence of L_{AB} on a_W remains, however, unchanged (compare Figure 6 with Figure SI-2 of Supporting Information where the L_{AB} values have been corrected for the direct recombination).

Combined Effect of T and a_W. Inspection of the best-fit parameters listed in Tables 1 and 2 indicates that the fraction of RCs competent for the $P^+Q_A^-Q_B \rightarrow P^+Q_AQ_B^-$ electron transfer ($1 - P_F$) remains essentially unchanged upon varying T and cosolute concentration. The same holds for the spread σ

(50) Indicating the sample volume as V_{tot}, one can write $n_S = [S]V_{tot}$ and $n_W = (V_{tot} - n_S v_S)/v_W$, from which eq 12 is easily obtained.

(51) Timasheff, S. N. *Proc. Natl. Acad. Sci. U.S.A.* **2002**, *99*, 9721.
(52) Labahn, A.; Bruce, J. M.; Okamura, M. Y.; Feher, G. *Chem. Phys.* **1995**, *197*, 355.
(53) Schmid, R.; Labahn, A. *J. Phys. Chem. B* **2000**, *104*, 2928.

of rate constants. Because both parameters are expected to be related to the availability of quinone at the Q_B-site (see the Supporting Information), this implies that, under conditions of high quinone loading, the degree of saturation of the Q_B-site remains constant. What is drastically affected by the cosolute and by the temperature is the average rate constant of $P^+Q_AQ_B^-$ charge recombination, λ. According to eq 3, λ depends on the interquinone electron transfer equilibrium constant L_{AB}. The T-dependence of L_{AB} is consistent with an enthalpy change that is only slightly dependent on composition (see Figure 4), and the results of the previous section strongly suggest an osmotic effect. Of course, addition of a solute modifies a plethora of chemical-physical parameters potentially relevant for electron transfer (e.g., dielectric constant, H-bonding degree, polarizability). Rather than quantifying the weight of all of these (unknown) changes, we will use an "Occam's razor" argument showing how all of the data of the present paper could be brought back to the dependence of the $P^+Q_A^-Q_B \leftrightarrow P^+Q_AQ_B^-$ equilibrium constant on temperature and water activity.

Let us consider as a reference state that of RCs in dilute buffer ($\ln(a_W) \approx 0$) at the temperature T_0. Because the activity of water a_W in solutions of glycerol and sugars has a negligible dependence on the temperature,[54] L_{AB} responds to changes in temperature and water activity according to:

$$d \ln L_{AB}(T, a_W) = \left(\frac{\partial \ln L_{AB}}{\partial T}\right)_{\ln(a_W)=0} dT + \left(\frac{\partial \ln L_{AB}}{\partial \ln(a_W)}\right)_{T_0} d \ln(a_W) \quad (14)$$

The two partial derivatives are given by the van't Hoff relationship ($\partial \ln L_{AB}/\partial T) = \Delta H_{AB}^\circ/RT^2$ and by eq 9, so that eq 14 can be easily integrated obtaining:

$$\ln L_{AB} = \ln L_{AB}^\circ + \frac{\Delta H_{AB}^\circ}{RT_0} + F(T, a_W) \quad (15)$$

where the function $F(T, a_W)$ of temperature and water activity is

$$F(T, a_W) = \Delta N_{exc,W} \ln(a_W) - \frac{\Delta H_{AB}^\circ}{RT} \quad (16)$$

Strictly, also ΔH_{AB}° could depend on the solution composition, but the results of Figure 4 suggest that it should vary only slightly in the presence of the cosolutes used in the present study. Under the simplifying assumption that $\Delta H_{AB}^\circ = -15$ kJ mol^{-1} (see Figure 4 and ref 39) holds independently from the solution composition while $\Delta N_{exc,W} = -3$ in the presence of glycerol and glucose and $\Delta N_{exc,W} = -6$ in the presence of disaccharides, we have evaluated the function $F(T, a_W)$ for each sample of Tables 1 and 2. As shown in Figure 7, all of the L_{AB} values determined in the present work follow essentially the same linear relationship when plotted in a semilog plot against the function $F(T, a_W)$. Figure 7 demonstrates that the dependence of the $P^+Q_A^-Q_B \leftrightarrow P^+Q_AQ_B^-$ equilibrium on temperature and water activity is sufficient to account satisfactorily for the behavior of $P^+Q_AQ_B^-$ charge recombination in the presence of different cosolutes, which affect substantially the chemico-physical properties of the solution. Other environmental variables are expected to play a minor role (if any).

Conformational Changes and Electron Transfer. Qualitative indications that high concentration of osmolytes (in particular, glycerol and ethylene glycol) somehow slows down the kinetics of $P^+Q_AQ_B^-$ charge recombination are hidden in the literature,[12,55,56] but this aspect has never been addressed in detail. Addition of glycerol (65 wt %) does not affect the direct charge recombination rates from the primary quinone (k_{AP}; see Figure 3) and secondary quinone (k_{BP}; see above and Supporting Information). The same holds when comparing results obtained in buffer[57] and glycerol[53] on a series of mutant RCs that span a wide range of free energy gap between the charge-separated states and the neutral (PQ_AQ_B) state (see also the Supporting Information). This indicates that the driving forces and the reorganization energies relevant for the $P^+Q_A^- \rightarrow PQ_A$ and $P^+Q_B^- \rightarrow PQ_B$ direct electron transfer are not influenced by the presence of high glycerol concentration. In turn, this implies that the free energy gap between the reduced primary and secondary quinones is independent of the water activity. At variance, we have shown here that the apparent equilibrium constant L_{AB} depends strongly on a_W with an apparent $\Delta N_{exc,W} \approx -3$ (e.g., upon addition of 65 wt % glycerol L_{AB} increases by 300%). Of course, this is incompatible with the sequence of processes described in reaction 2 that links the L_{AB} value to the free energy gap between the $P^+Q_A^-Q_B$ and the $P^+Q_AQ_B^-$ states ΔG_{AB}° ($L_{AB} = \exp(-\Delta G_{AB}^\circ/RT)$. The observed strong osmolyte-induced increase in L_{AB} at constant ΔG_{AB}° can be explained only assuming the presence of at least one additional step connecting the initial (flash-induced) $P^+Q_A^-Q_B$ state and the final $P^+Q_AQ_B^-$ state. To account for the observed strong a_W-dependence of the rate of $P^+Q_AQ_B^-$ recombination, this step must involve the release of water molecules and likely some conformational changes of RC. Such a minimal scheme has two options: (i) the conformational step precedes the electron transfer, which could be thus conformationally gated; (ii) the conformational step follows the electron transfer (postelectron transfer relaxation). It was already demonstrated that the rate of electron transfer from the primary to the secondary quinone is independent of the associated redox free energy change, suggesting, on a kinetic basis, a conformational gating,[13] but the nature of such a gating is still unresolved. Reaction 17 represents a conformational gating of electron transfer (for the sake of simplicity, the direct recombination from Q_B^- has been neglected, but it can be easily included without changing the results).

$$(P^+Q_A^-Q_B)\alpha \overset{K_{conf}}{\longleftrightarrow} (P^+Q_A^-Q_B)\beta - \Delta N_W H_2O \overset{K_{ET}}{\longleftrightarrow} (P^+Q_AQ_B^-)\beta - \Delta N_W H_2O \quad (17)$$

The protein can exist in two different states labeled as α and β. In the α state, the electron transfer to Q_B is impaired, and only direct recombination from Q_A^- is allowed. On the contrary, in the β state, the $Q_A^-Q_B \rightarrow Q_AQ_B^-$ electron transfer can proceed. The release of buried water molecules ($\Delta N_{exc,W} = \Delta N_W$) associated with the $\alpha \rightarrow \beta$ transition was written as $-\Delta N_W$ according to the formalism of reaction 6 (in the present case, $-\Delta N_W$ is positive). The equilibrium constants for the conformational and electron transfer steps are defined as $K_{conf} = [(P^+Q_A^-Q_B)\beta]a_W^{-\Delta N_W}/[(P^+Q_A^-Q_B)\alpha]$ and $K_{ET} = [(P^+Q_AQ_B^-)\beta]/[(P^+Q_A^-Q_B)\beta]$. To fulfill the experimental effect of a_W, the

(54) He, X.; Fowler, A.; Toner, M. *J. Appl. Phys.* **2006**, *100*, 074702.
(55) Tiede, D. M.; Vazquez, J.; Cordova, J.; Marone, P. A. *Biochemistry* **1996**, *35*, 10763.
(56) Larson, J. W.; Wraight, C. A. *Photosynth. Res.* **1995**, 65.
(57) Allen, J. P.; Williams, J. C.; Graige, M. S.; Paddock, M. L.; Labahn, A.; Feher, G.; Okamura, M. Y. *Photosynth. Res.* **1998**, *55*, 227.

recombination from Q_A^- is assumed to occur only in the α state (see below). Under this assumption, the rate constant for $P^+Q_AQ_B^-$ recombination through repopulation of the $(P^+Q_A^-Q_B)\alpha$ state is given by the k_{AP} rate constant weighted for the relative occupancy of the $(P^+Q_A^-Q_B)\alpha$ state:

$$\lambda = k_{AP}\frac{(P^+Q_A^-Q_B)\alpha}{(P^+Q_A^-Q_B)\alpha + (P^+Q_A^-Q_B)\beta + (P^+Q_AQ_B^-)\beta} \tag{18a}$$

that is,

$$\lambda = k_{AP}\frac{1}{1 + K_{conf}a_W^{\Delta N_w}(1 + K_{ET})} \tag{18b}$$

According to eq 18b, evaluation of L_{AB} through eq 5 yields:

$$L_{AB} = K_{conf}a_w^{\Delta N_w}(1 + K_{ET}) \tag{19}$$

The above equation well accounts for the experimental dependence of L_{AB} on water activity ($d \ln(L_{AB})/d \ln(a_W) = \Delta N_W$; cf., eq 9) and clarifies how L_{AB} is not linked directly to the free energy gap of the overall process $\Delta G_{AB}^\circ = RT \ln(K_{conf}K_{ET})$. Note that the cases in which the recombination from Q_A^- occurs in the β state or in both the α and the β states lead to dependencies of L_{AB} on a_W different from eq 9.[58,59] According to the hypothesis of a conformational gating, the rationale of the independence of L_{AB} on ΔG_{AB}° is shown in the energy diagram of Figure 7; the osmotic effect acts on the free energy level of the intermediate state $(P^+Q_A^-Q_B)\beta$ leaving unchanged the two extreme states.

A minimal scheme for postelectron transfer relaxation is:

$$(P^+Q_A^-Q_B)\alpha \xleftrightarrow{K_{ET}} (P^+Q_AQ_B^-)\alpha \xleftrightarrow{K_{conf}} (P^+Q_AQ_B^-)\beta - \Delta N_W H_2O \tag{20}$$

In this case, there are no ambiguities on the RC state involved in the recombination from Q_A^-, and the L_{AB} evaluated through eq 5 becomes $L_{AB} = K_{ET} + K_{conf}a_W^{\Delta N_W}$. Such a relation, although leading to a nonlinear dependence of $\ln(L_{AB})$ on $\ln(a_W)$, describes reasonably the glycerol data of Figure 6A with a $\Delta N_W = -5 \pm 1$ (not shown). The very small a_W-range explored with trehalose does not allow a reliable fit of data to this relationship. Note that according to reaction 20 the free energy level of the final state depends on a_W. This in principle would exclude the postelectron transfer relaxation model, unless direct recombination of the $P^+Q_AQ_B^-$ state occurs mainly from the nonrelaxed state, whose free energy level is not affected by the water activity.

Thus, irrespective of the model adopted (eq 17 or eq 20), our data indicate, on a thermodynamical ground, the presence of a conformational transition associated with the electron transfer from Q_A^- to Q_B and coupled with the release of few water molecules. In the discussion leading to scheme 17, we have labeled as conformational the process preceding the final electron transfer. This is because there is a general consensus on the involvement of conformational changes in the kinetics of formation and stability of the semiquinone at the Q_B site (for example, RC in the $P^+Q_AQ_B^-$ state shows an increased susceptibility to protease cleavage).[60] Reaction 17 holds independently of the nature of the two equilibria involved, and thus it could formally accommodate the outcome of a recent FTIR study where the appearance of Q_B^- and the disappearance of Q_A^- have been found to be decoupled.[61] On the basis of this observation, the existence of an intermediate electron donor/acceptor and of two sequential electron transfer steps has been proposed according to a scheme ($P^+Q_A^-Q_BX \leftrightarrow P^+Q_A^-Q_B^-X^+ \leftrightarrow P^+Q_AQ_B^-X$) that is formally equivalent to eq 17 if the formation of $P^+Q_A^-Q_B^-X^+$ is coupled to the release of $-\Delta N_W$ water molecules. However, a subsequent investigation[62] provided evidence against the presence of the putative electron acceptor X. In the absence of an unambiguous indication of the existence of X and of the associated nonorthodox pathway for formation of $P^+Q_A^-Q_B^-$, we will limit the following discussion to the linkage between conformational changes and electron transfer processes.

Implications. Osmotic effects on the functionality of biomolecules have been widely recognized in processes involving ligand/substrate binding, membrane channels, and interprotein interactions.[31,47] On the contrary, indications on the influence of water activity on intraprotein electron transfer were limited to the case of the water cycle of *cytochrome c oxidase*.[63] According to the above-discussed data, the intraprotein electron transfer from Q_A^- to Q_B, within the RC, is linked to the release of 3−4 water molecules (the exact number depends on the relevance of direct recombination from Q_B^-). Because such an effect is observed with small size osmolytes such as glycerol, it is likely that osmotic stress acts on water secluded in cavities sterically inaccessible to the solute. The equilibrium for the overall $P^+Q_A^-Q_B \leftrightarrow P^+Q_AQ_B^-$ process is strongly influenced by the water activity, while the rates of direct charge recombination from $P^+Q_A^-$ and $P^+Q_AQ_B^-$ (k_{AP} and k_{BP}, respectively) are insensitive to a_W. This implies that the interquinone electron transfer involves at least two RC substates (labeled as α and β in the previous section) differing in the stoichiometry of (solute-inaccessible) interacting water molecules. In principle, the α → β transition could either precede (gating, eq 17) or follow (relaxation, eq 20) the electron transfer, but, as described in the previous section, the independence of k_{BP} on the water activity favors the former scheme. Of course, the osmotic stress experiments of the present investigation do not allow one to identify which water molecules influence the stability of the intermediate RC substate, but the high-resolution crystal structure of RCs from *Rb. sphaeroides* reveals many buried water molecules, some of which are well positioned for playing a role in the events associated with the $P^+Q_A^-Q_B \leftrightarrow P^+Q_AQ_B^-$ electron transfer.[14,15,64,65] A role of internal water molecules in the proton transfer events associated with the electron transfer has been considered in previous FTIR studies,[66,67] but the concept of a significant contribution of water release to the RC

(58) In the case of direct recombination from $(P^+Q_A^-Q_B)\beta$, $L_{AB} = K_{ET} + a_W^{-\Delta N_W}/K_{conf}$; in the case of Q_A^- recombination from both β and α states, $L_{AB} = K_{ET}/(1 + a_W^{-\Delta N_W}/K_{conf})$.

(59) Note also that in the case of recombination from $(P^+Q_A^-Q_B)$ β state, the slowing of λ should reflect an increased population of the unproductive $(P^+Q_A^-Q_B)$ α state at the expense of the $(P^+Q_AQ_B^-)$ β state. Thus, we expect, upon addition of osmolytes, a decrease in the yield of Q_B^- that was never observed.

(60) Brzezinski, P.; Andreasson, L. E. *Biochemistry* **1995**, *34*, 7498.
(61) Remy, A.; Gerwert, K. *Nat. Struct. Biol.* **2003**, *10*, 637.
(62) Breton, J. *Biochemistry* **2007**, *46*, 4459.
(63) Kornblatt, J. A.; Kornblatt, M. J. *Biochim. Biophys. Acta* **2002**, *1595*, 30.
(64) Ermler, U.; Fritzsch, G.; Buchanan, S. K.; Michel, H. *Structure* **1994**, *2*, 925.
(65) Friztch, G.; Kampmann, L.; Kapaun, G.; Michel, H. *Photosynth. Res.* **1998**, *55*, 127.
(66) Breton, J.; Nabedryk, E. *Photosynth. Res.* **1998**, *55*, 301.

conformational changes is new. The nature of the conformational changes associated with the intra-RC electron transfer is still an open question. An obvious candidate for the $(P^+Q_A^-Q_B)\alpha \rightarrow (P^+Q_A^-Q_B)\beta$ transition described in reaction 17 is the movement of Q_B from the distal to the proximal position (see Introduction). Such a movement clearly favors the interquinone electron transfer and could be reasonably associated with the flux of some water molecules displaced by the quinone headgroup (Q_B in the proximal position replaces two water molecules that could stay between Glu-L212 and His-L190 when it is in the distal position).[14] Moreover, in RC crystals frozen in the presence of glycerol or ethylene glycol, Q_B occupies mainly the proximal site, while in the absence of osmolytes the room temperature structures showed that Q_B is mainly in the distal position.[68] Unfortunately, this last evidence carries some ambiguities: crystals were not stable in the presence of osmolytes at room temperature.[68] The distal-to-proximal movement of Q_B was already proposed as the conformational gate,[13,14] but arguments against its role as the rate-determining step accumulated in the past decade.[16–18,69] Recent studies suggest that, while the movement to the proximal site is necessary for the $Q_A^-Q_B \rightarrow Q_AQ_B^-$ electron transfer, the gating is accomplished by an unidentified protein response.[70] We propose that the observed release of water upon electron transfer reflects this response and that osmotic stress can properly tune it. This hitherto neglected role of water activity could have far-reaching implications in the design of future experiments dedicated to unravel the interplay among structure, dynamics, and functionality of RC.

Comparison with our recent studies[19,21] indicates that the substates involved in the $Q_A^-Q_B \rightarrow Q_AQ_B^-$ electron transfer are not limited to those probed here by osmotic stress (i.e., α and β). In the presence of trehalose at concentration larger than 50 wt %, the sample becomes supercooled and very viscous, and undergoes a glass transition above about 90 wt %.[71] We have observed[21] that the rate of charge recombination λ does not change appreciably across the glass transition (see also Table 2) and consequently the linear dependence of $\ln L_{AB}$ on $\ln(a_W)$ breaks down (Figure 6A). This is not unexpected because the transformation of the environment into a rigid solid matrix suppresses any water flow and thus any osmotic effect. However, in (amorphous) solid samples, another effect arises: the electron transfer from Q_A^- to Q_B is progressively blocked in a fraction of RCs.[19,21] The extent of this block depends somehow on the nature of the matrix (likely on its rigidity), but the rate of charge recombination remains essentially unaffected.[21–23] This behavior is apparent also in the data of Table 2. In fact, in liquid solution (48 wt % trehalose), almost all of the RCs (95%) undergo $P^+Q_AQ_B^-$ charge recombination with a rate constant $\lambda = 0.49$ s^{-1}, and these features remain essentially unchanged in a "wet" glass (90 wt % trehalose). On the contrary, in a "dry" glass (94.5 wt % trehalose) the fraction of RCs recombining from $P^+Q_AQ_B^-$ (with a slightly lower rate $\lambda = 0.41$ s^{-1}) drops to 54%. These and other results (obtained on RCs embedded into several solid matrices)[19,20] indicate the existence of two additional RC conformations. In one conformation ("active"), electron transfer to Q_B takes place, while in the other one ("inactive") the interquinone electron transfer is drastically inhibited and only recombination of the $P^+Q_A^-$ state is observed. The increase in P_F and the steadiness of λ observed upon increasing the rigidity of the surroundings reflect the heterogeneous hindering of the "active" to "inactive" conformational transition, which leaves unchanged L_{AB} and thus the conformational equilibrium probed by osmotic stress. On the other hand, in liquid solution the competence of RCs for interquinone electron transfer is independent of the cosolute nature and concentration ($P_F \sim$ constant; see Tables 1 and 2) providing evidence that in these liquid systems the "active" $\leftrightarrow$ "inactive" conformational equilibrium remains unchanged while L_{AB} is strongly affected by osmotic dehydration. As a whole, these data indicate that there are at least two transitions involved in the overall $Q_A^-Q_B \rightarrow Q_AQ_B^-$ electron transfer process. A first conformational transition ("inactive" $\rightarrow$ "active") is the essential prerequisite for the electron transfer step and is blocked when the protein surface is locked by hardening of the surrounding matrix.[19] The second conformational change ($\alpha \rightarrow \beta$), coupled to the release of about three water molecules, occurs in RCs that are still competent for the interquinone electron transfer and can be tuned by changing the solution osmotic pressure.

Acknowledgment. The financial support of MIUR of Italy is acknowledged (grant COFIN-PRIN/2005 prot. 2005027011 and funds associated with the proposal COFIN-PRIN/2007 prot. 2007WTJEY5). G.P., F.L., and M.G. were partially supported by the Consorzio Interuniversitario per lo sviluppo dei Sistemi a Grande Interfase (CSGI-Firenze).

Supporting Information Available: Implications of the quinone exchange between the Q_B site of the RC and the detergent domain, and contribution of direct $P^+Q_AQ_B^-$ recombination to the evaluation of L_{AB}. This material is available free of charge via the Internet at http://pubs.acs.org.

JA801963A

(67) Hermes, S.; Stachnik, J. M.; Onidas, D.; Remy, A.; Hofmann, E.; Gerwert, K. *Biochemistry* **2006**, *45*, 13741.
(68) Pokkuluri, P. R.; Laible, P. D.; Crawford, A. E.; Mayfield, J. F.; Yousef, M. A.; Ginell, S. L.; Hanson, D. K.; Schiffer, M. *FEBS Lett.* **2004**, *570*, 171.
(69) Breton, J. *Biochemistry* **2004**, *43*, 3318.
(70) Paddock, M. L.; Flores, M.; Isaacson, R.; Chang, C.; Abresch, E. C.; Selvaduray, P.; Okamura, M. Y. *Biochemistry* **2006**, *45*, 14032.
(71) Miller, D. P.; de Pablo, J. J.; Corti, H. *Pharm. Res.* **1997**, *14*, 578.